JOURNAL OF APPLIED ELECTROCHEMISTRY **27** (1997) 469–476

Mass transfer in an annular electrodialysis cell in pulsating flow

J. GARCÍA-ANTÓN, V. PÉREZ-HERRANZ, J. L. GUIÑÓN

Departamento de Ingeniería Química y Nuclear, E.T.S.I. Industriales, Universidad Politécnica de Valencia, PO Box 22012. 46071, Valencia, Spain

Received 10 June 1996; revised 20 August 1996

The effect of pulsating flow on the mass transfer in an annular electrodialysis cell has been studied in terms of the limiting current. The results indicate that the limiting current is influenced by the fluid velocity, the pulsation amplitude and the pulsation frequency, giving an increase of 400% with respect to the steady state. For a given amplitude, the dimensionless velocity, α_0 ($\alpha_0 = a\omega/v$), can be taken as a representative parameter of the pulsation effect on the mass transfer. The fractional increase in the Sherwood number in pulsating flow with respect to the steady state has been correlated in terms of the dimensionless velocity, α_0, and the Stokes number, α_1 ($\alpha_1 = D_{eq}\,(\omega/v)^{1/2}$), giving the correlation:

$$\frac{Sh_p - Sh_0}{Sh_0} = 0.192(\alpha_0\alpha_1)^{0.377}$$

List of symbols

a	pulsation amplitude (m)
C_0	bulk concentration (mol m^{-3})
D	diffusion coefficient or diffusivity of chromate ions (m^2 s^{-1})
D_{eq}	equivalent diameter of electrodialysis cell (m)
F	Faraday constant (96 500 C mol^{-1})
I	current (A)
$\bar{I}$	time averaged current (A)
I_0	limiting current in steady flow (A)
I_p	limiting current in pulsating flow (A)
I_{lim}	limiting current (A)
k_p	mass transfer coefficient in pulsating flow (m s^{-1})
k_0	mass transfer coefficient in steady flow (m s^{-1})
R_1	radius of the inner cylinder (m)
R_2	radius of the outer cylinder (m)
S	membrane surface exchange area (m^2)
Sh	Sherwood number ($I_{lim}\ D_{eq}$ / $S\ z\ F\ D\ C_0$)
Sh_0	Sherwood number in steady flow
Sh_p	Sherwood number in pulsating flow
U	cell voltage (V)
v	fluid velocity (m s^{-1})
z	Electrochemical valence

Greek letters

α_0	dimensionless velocity ($a\ \omega / v$)
α_1	Stokes number $D_{eq}\ (\omega / v)^{1/2}$
$\Delta\phi$	instantaneous voltage drop across the membrane (V)
$\Delta\bar{\phi}$	time averaged voltage drop across the membrane (V)
λ^0	equivalent conductance at infinite dilution (cm^2 s equiv^{-1})
ν	kinematic viscosity (m^2 s^{-1})
ρ	density (kg m^{-3})
ω	pulsation frequency (s^{-1})

1. Introduction

Electrodialysis is one of the techniques that can be used for the treatment of acid effluents from industry. Using this process, concentrated acid can be obtained with anion exchange membranes showing a low permeability for protons. Electrodialysis has the advantage over other techniques that it can operate as a continuous process, and does not need any regeneration steps, which generally yield about the same volume of liquid wastes as the solution treated [1, 2].

The recovery of acids by electrodialysis can be performed with sulfuric acid [3–9], hydrochloric acid [10–12], phosphoric acid [13] and chromic acid [14–16]. With chromic acid, some studies have been carried out to improve the electrodialysis efficiency. For this purpose, Catonne and Royon [14] studied the application of electro-electrodialysis to the recovery of chromic acid from rinsing baths in the electroplating industry. They took CrO_3, with a concentration of 100 g dm^{-3}, ready to use in the electroplating bath, from a solution of 20 g dm^{-3} in CrO_3 in the rinsing bath. Cohen and Duclert [16], used ARA anionic membranes produced by Morgane™ for the same purpose, obtaining a concentration of 323 g dm^{-3} CrO_3 from an initial concentration of 8 g dm^{-3} CrO_3.

Although ion exchange membrane electrodialysis systems are better operated at high current densities, the operational current density must be kept below

the limiting current density to avoid water electrolysis, pH changes in the solution, electrical noise and increase in the electrical resistance of the cell. These phenomena occur in the diluting compartment, since it is in this compartment that mass transfer is taking place. The limiting current densities increase as the solution concentration, flow rate, temperature, ion mobility and diffusivity increase.

The effect of hydrodynamics, including laminar and turbulent flows, on ionic mass transfer by electrodialysis has been studied by many researchers, where the Sherwood number is correlated with the Reynolds number, the Schmidt number and the dimensionless hydraulic equivalent diameter. In this way, in laminar flow, the Sherwood number varies with the Reynolds number following a one third power law, but in turbulent flow the exponent is 0.8 [17–20].

One method of increasing mass transfer rates is to superpose an oscillating flow to the steady flow. Gibert and Angelino [21, 22] and Guiñón *et al.* [23] studied the effect of pulsating flow on mass transfer between a sphere and a liquid. Krasuk and Smith studied mass transfer in a pulsed column [24]. Mackley and Ni [25] and Harrison and Mackley [26] studied the effect of pulsating flow on mass transfer in a pulsating flow bioreactor. Finally, mass transfer in a particle bed with oscillating flow was studied by Krasuk and Smith [27], Ratel *et al.* [28] and Coeuret and Paulin [29]. From this work it can be concluded that, in general, the pulsating flow enhances mass transfer.

This paper deals with the effect of pulsating flow on mass transfer in an annular pulsating electrodialysis cell, applied to the recovery of chromic acid from the rinsing baths of eletroplating industries. Mass transfer was studied in terms of the limiting current which was determined by following the Cowan and Brown method [30]. The effect of pulsation on the limiting current was investigated by varying the frequency and amplitude of pulsations at different velocities. Finally, the relative variation of mass transfer across the anionic membrane was correlated in terms of the dimensionless groups α_0 and α_1, where α_0 is the dimensionless velocity, and α_1 is the Stokes number:

$$\alpha_0 = a\omega/v \tag{1}$$

$$\alpha_1 = D_{eq}\sqrt{\omega/v} \tag{2}$$

These dimensionless groups are representative of the hydrodynamics in pulsating flow and are obtained from the theoretical solution of the momentum balance in pulsating flow for different geometries such as circular pipes [31], annuli [32] and packed beds [33]. These dimensionless groups have been used in the study of mass transfer in pulsating flow in an empty column [24] and in packed beds [27, 28].

The dimensionless velocity, α_0, represents the ratio of the amplitude of the velocity in pulsating flow to the time-average velocity [24]. On the other hand, the Stokes number, α_1, is a measure of the intensity of the flow oscillations [33].

2. Experimental details

The chemical system chosen for this work was a solution of chromate ions from a bath whose concentration, C_0, was 9.62×10^{-3} M CrO_3 and 0.05 M H_2SO_4. These concentrations are equivalent to those of the rinsing baths in the electroplating industry. The solution was prepared by dissolving ACS certified reagent grade chemicals in distilled water. The physical properties of the electrolyte at 25 °C were as follows: density, $\rho = 1000.8\,kg\,m^{-3}$ and kinematic viscosity, determined using a Cannon Fenske viscosimeter, $v = 1.13\times10^{-6}\,m^2\,s^{-1}$. The diffusivity of chromate ions, calculated from the equivalent conductance at infinite dilution, λ^0, by means of the Nernst equation [34], was $D = 11.34\times10^{-10}\,m^2\,s^{-1}$. The solution used was the same in the two sections of the annular electrodialysis cell, in order to minimize diffusion problems through the membrane owing to concentration gradients on the two sides of the membrane.

The experimental arrangement used in this work is shown in Fig. 1. The electrodialysis cell consists of a Plexiglas outer tube, 30 cm long with a 4 cm inner radius R_2, and a cylindrical PVC framework, 25 cm long, with a 2 cm outer radius R_1, to support the anionic membrane. This assembly, framework–membrane, separates the cell into two concentric cylinders. The outer cylinder, which acts as the cathodic dilution compartment, is where concentration polarization phenomena can occur. The inner cylinder acts as the anodic compartment, or concentration compartment. The membrane used in this work was the ARA 17–10 membrane produced by Morgane™. This membrane is specially designed for the recovery of acids by electrodialysis. The membrane area was 250 cm^2.

Before utilization, the membranes were soaked in a 0.05 M H_2SO_4 solution, and before the experiments, the membranes were preconditioned for 24 h with the same solution of CrO_3 used in the experiments. The membrane exchange capacity was 0.60 mequiv g^{-1} of dry membrane [1].

The cathode was a 7 cm diameter and 20 cm high AISI 316 stainless steel cylindrical grid. The anode was a 20 cm high lead-antimony (10% Sb) bar.

Below the cell, a 15 cm high calming section filled with 3 mm diameter glass spheres was provided. The calming section was separated from the cell by a grid to prevent any fluidization phenomena in the bed.

Pulsation was produced by means of deformable PTFE membrane inside a tube with the same diameter as the cell, which acted as a piston. The motor rotation motion was transformed into translation motion by a crankshaft system. To convert the cyclic output of the transmission into a back-and-forth movement of the piston, a coupling mechanism was used. The pulsation amplitude was modified by

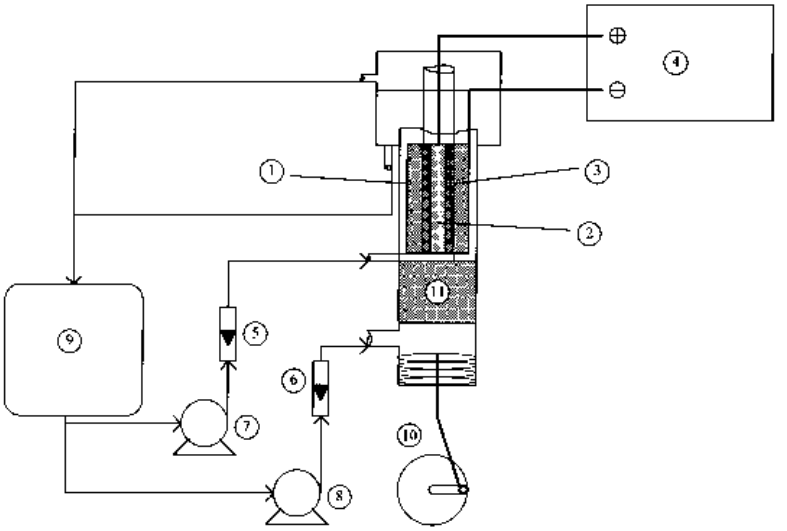

Fig. 1. Flow diagram of the experimental arrangement. Key: (1) cathode, (2) anode, (3) membrane, (4) power supply, (5) and (6) rotameters, (7) and (8) pumps, (9) storage tank, (10) pulsation system and (11) calming section.

changing the length of the connecting rod. The pulsation frequency was modified by changing the motor rotation speed.

The major independent variables investigated were fluid velocity, v, pulsation frequency, ω, and pulsation amplitude, a, which were varied in the following ranges:

$$1.33 \times 10^{-3}\,\mathrm{m\,s^{-1}} \leq v \leq 6.63 \times 10^{-3}\,\mathrm{m\,s^{-1}}$$

$$0\,\mathrm{s^{-1}} \leq \omega \leq 2\pi\,\mathrm{s^{-1}}$$

$$2 \times 10^{-3}\,\mathrm{m} \leq a \leq 8 \times 10^{-3}\,\mathrm{m}$$

The limiting current was determined using the Cowan and Brown method [30]. This method consists of plotting resistance, $\Delta\phi/I$, against the inverse of current, $1/I$, where $\Delta\phi$ is the voltage drop across the membrane and I is the current. The limiting current, I_{lim}, corresponds to a minimum in this plot. The variations of the limiting current are obtained with an accuracy of about 8% due to the difficulty of determining it. Data were occasionally erratic probably because of changes on the membrane surface throughout the experiments when the limiting current is exceeded. To determine the values of the current and the voltage drop across the membrane a constant cell voltage, U, was applied using a regulated d.c. power supply. Once the cell voltage was fixed, and the current established, the current and voltage drop across the membrane were measured. The cell voltage was then increased and the process repeated until the number of measured points of I and $\Delta\phi$ were sufficient to determine the limiting current.

The experimental arrangement used to measure the voltage drop through the membrane and the current is shown in Fig. 2. The voltage drop was measured using two graphite probes near the two membrane/solution interfaces. A data acquisition system with a typical conversion time of 25 μs was used to measure the variation of voltage drop through the membrane and current with time. The

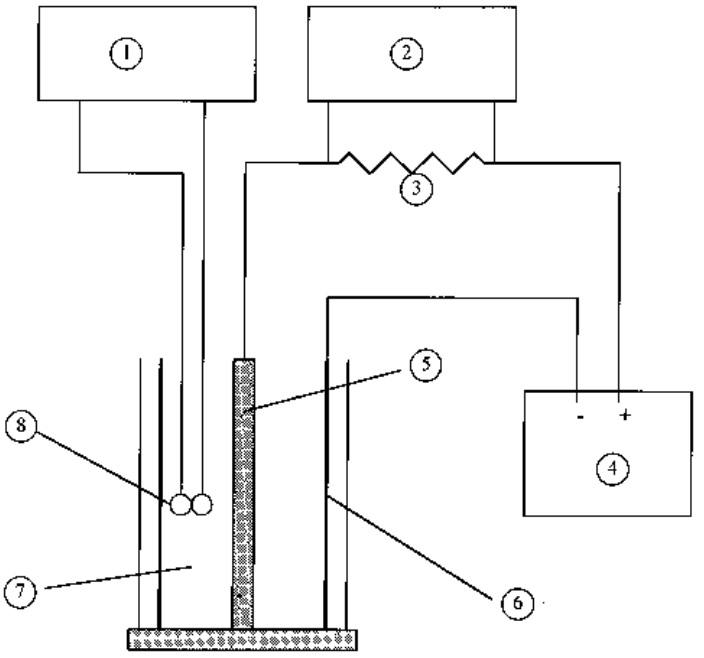

Fig. 2. Flow diagram of the experimental arrangement used to determine the limiting current. Key: (1) potential register, (2) current register, (3) resistance (0.1 Ω), (4) power supply, (5) anode, (6) cathode, (7) membrane and (8) graphite probes.

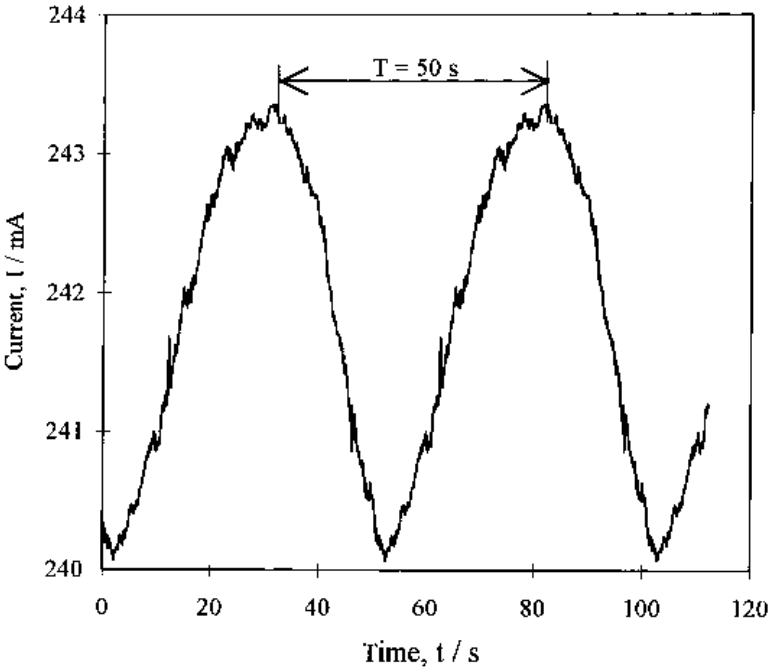

Fig. 3. Experimental variation of the instantaneous value of the current with time. Case of nonreversing flow. $a = 0.008$ m, $\omega = 0.123\ s^{-1}$, $v = 98 \times 10^{-3}\ m\ s^{-1}$.

cell voltage was fixed using a Gossen Konstanter SSP stabilized d.c. power supply.

3. Results

3.1. *Effect of pulsating flow on the instantaneous value of the current*

The change in the instantaneous value of the shear stress on the membrane surface due to pulsations, corresponds to a change in the boundary layer thickness, and as a consequence of this, the instantaneous current I, changes with time, when operating at constant cell voltage, U.

Figures 3 and 4 show the variation of the instantaneous value of the current, I, with time for two different pulsation frequencies. From these figures, it can be concluded that in the case of nonreversing flow (Fig. 3.), the current, I, varies sinusoidally, with the same frequency as the fluid pulsations, but, in the case of reversing flow (Fig. 4), the current reaches two maxima and two minima in one pulsation cycle. Similar conclusions have been obtained by Guiñón *et al.* in [21] and Ratel *et al.* [26], studying the electrochemical reduction of copper in pulsating flow, at a sphere and in a packed bed electrode, respectively.

3.2. *Effect of pulsating flow on the limiting current*

In the case of pulsating flow, under certain hydrodynamic conditions, once the cell voltage is fixed, the

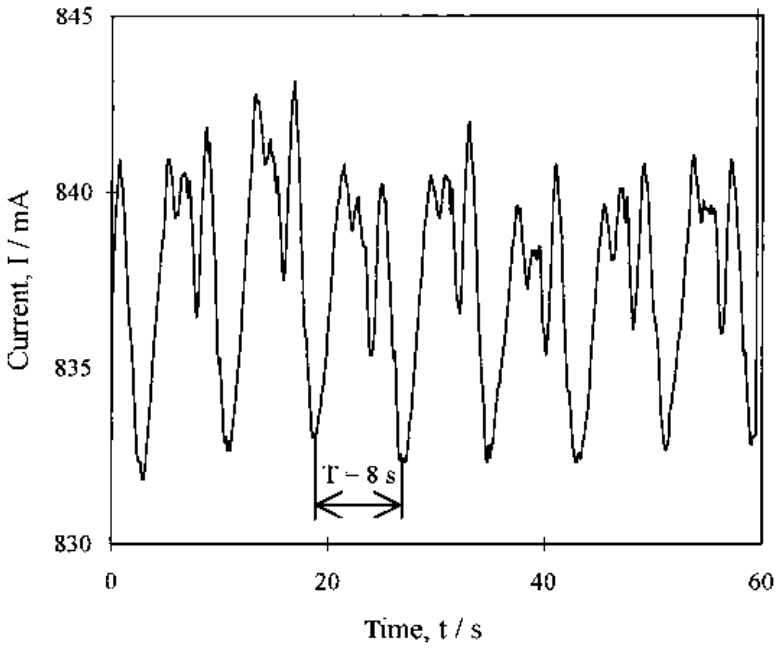

Fig. 4. Experimental variation of the instantaneous value of the current with time. Case of reversing flow, $a = 0.008$ m, $\omega = 0.79\ s^{-1}$, $v = 1.33 \times 10^{-3}\ m\ s^{-1}$.

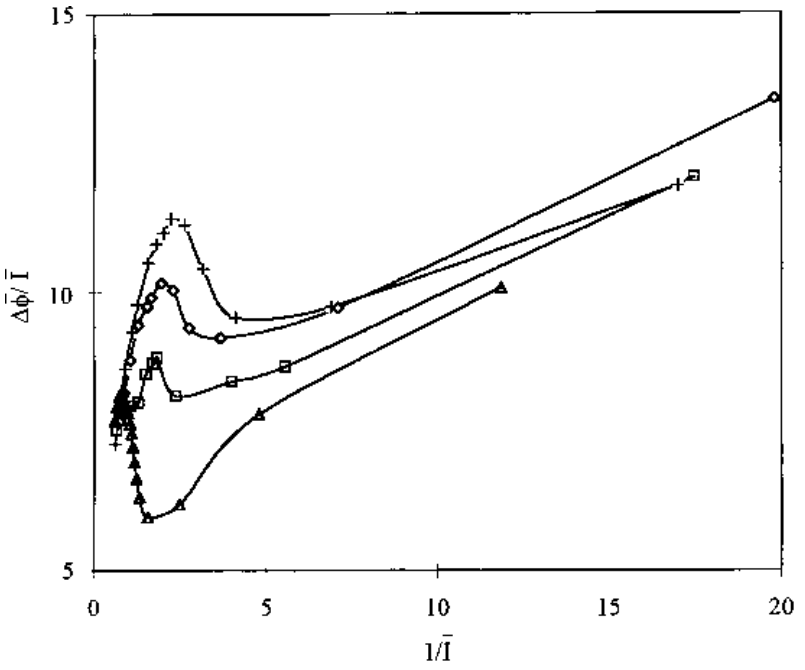

Fig. 5. Effect of pulsating flow on the curves $\Delta\bar{\phi}/\bar{I}$ against $1/\bar{I}$, for different values of the pulsation frequency. $a = 8\times10^{-3}$ m, $v = 6.63\times10^{-3}$ m s^{-1}. Key: (+) $\omega = 1.66$ s^{-1}, (◊) $\omega = 3.04$ s^{-1}, (□) $\omega = 4.54$ s^{-1} and (Δ) $\omega = 6.30$ s^{-1}.

current changes with time, as discussed before (Figs 3 and 4), but after a few minutes a quasisteady state is reached. Then, the instantaneous value of current, varies with time, but its time averaged value remains constant. These time averaged values of current, $\bar{I}$, and voltage drop, $\Delta\bar{\phi}$, for several pulsation cycles have been considered for the determination of the limiting current in pulsating flow, following the Cowan and Brown method [30].

Figures 5 and 6 show the effect of pulsating flow on the $\Delta\bar{\phi}/\bar{I}$ against $1/\bar{I}$ curves at different fluid velocities. It can be concluded that the limiting current increases with pulsation frequency as the minimum value of these plots, corresponding to the limiting current, shifts to lower values of $1/\bar{I}$ with increase in frequency. A further conclusion is that the resistance at the membrane–fluid interface decreases in pulsating flow, as the ratio $\Delta\bar{\phi}/\bar{I}$ decreases for a given value of current.

To illustrate the effect of pulsating flow on the limiting current with respect to the steady state, the variation of the ratio I_p/I_0 with the pulsation parameters, frequency, ω, and amplitude, a, and fluid velocity, v, was studied, I_p being the limiting current in pulsating flow and I_0, the limiting current in steady state. Figures 7 and 8 show the variation of the ratio I_p/I_0 with respect to frequency for different values of the steady velocity and amplitude, respectively. For a given amplitude, Fig. 7, the ratio I_p/I_0 decreases with velocity. This can be explained by the fact that the current I_0 increases with the velocity and, consequently, the influence of pulsation on the flow

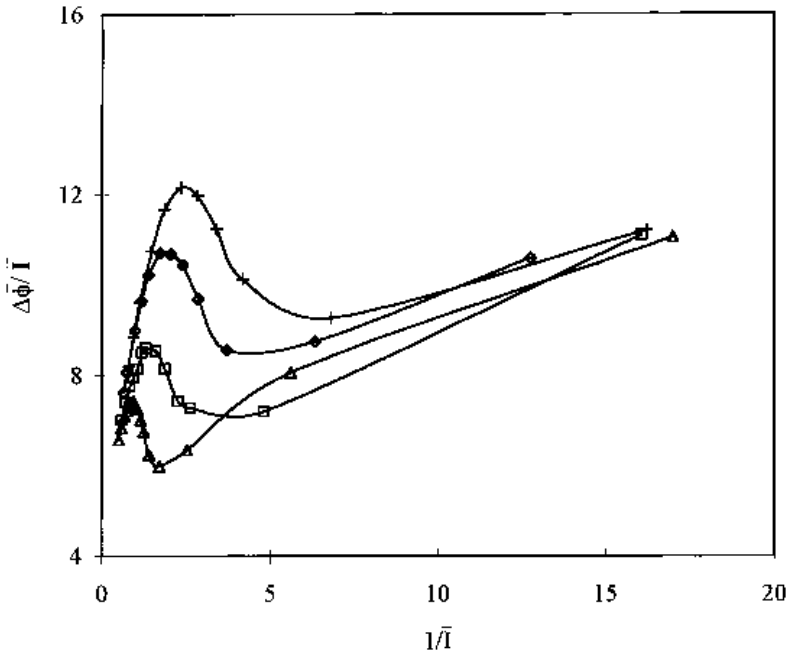

Fig. 6. Effect of pulsating flow on the curves $\Delta\bar{\phi}/\bar{I}$ against $1/\bar{I}$, against $1/\bar{I}$, for different values of the pulsation frequency. $a = 8\times10^{-3}$ m, $v = 3.98\times10^{-3}$ m s^{-1}. Key: (+) $\omega = 1.65$ s^{-1}, (◊) $\omega = 3.06$ s^{-1}, (□) $\omega = 4.61$ s^{-1} and (Δ) $\omega = 6.45$ s^{-1}.

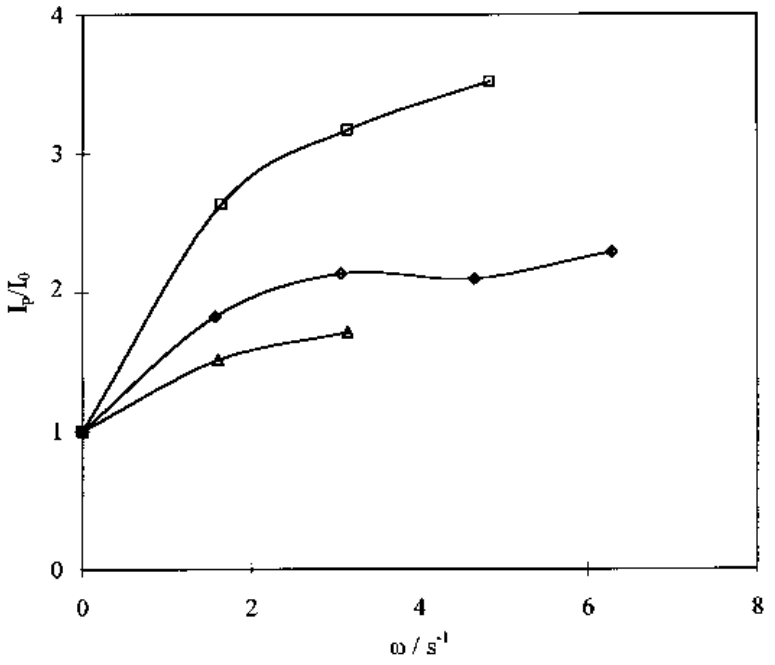

Fig. 7. Variation of the ratio I_p/I_0 with frequency for different values of the fluid velocity. $a = 0.002$ m. Key: (□) $v = 1.33\times10^{-3}$ m s^{-1}, (◊); $v = 3.98\times10^{-3}$ m s^{-1} and (Δ) $v = 6.63\times10^{-3}$ m s^{-1}.

structure decreases with an increase in velocity. On the other hand, for a given value of velocity, Fig. 8, I_p/I_0 increases with amplitude. This behaviour can be explained from the relative variation of the shear stress in an annular duct in pulsating flow, with respect to the steady state, since it decreases with velocity, and increases with frequency and amplitude, as can be concluded from the theoretical work of Perez-Herranz [32]. From these figures it can be concluded that pulsating flow can be used to obtain improved operational conditions in electrodialysis systems, as the limiting current increases with respect to the steady state.

In pulsating flow, reverse flow can take place for part of a cycle, when the dimensionless velocity (Equation 1), $\alpha_0 > 1$. If $\alpha_0 < 1$, pulsation is not large enough to cause reverse flow. In this case, pulsations have a negative effect on mass and heat transfer [23, 28, 35].

Figures 9 and 10 show the variation of I_p/I_0 with the dimensionless velocity, α_0, in the case of reversing flow ($\alpha_0 > 1$), for different values of the steady velocity and amplitude, respectively. Figure 9 shows that for a given value of amplitude, the dimensionless velocity, α_0, can be taken as a representative parameter of the pulsation effect on the limiting current, as the variation of I_p/I_0, is independent of the fluid velocity. On the other hand, as can be seen in Fig. 10, for a given velocity, the ratio I_p/I_0 decreases with amplitude. This behaviour is different from that found by Guiñón *et al.* [23] for mass transfer between a sphere and a liquid in pulsating flow. These authors found that for a given value of α_0, the mass transfer between a sphere and a liquid in pulsating flow decreases when

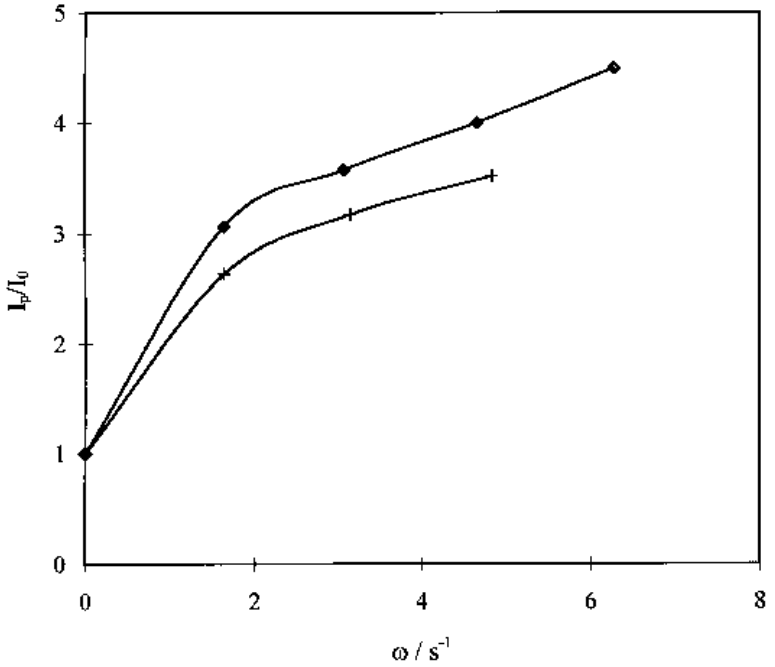

Fig. 8. Variation of the ratio I_p/I_0 with frequency for different values of the pulsation amplitude. $v = 1.33\times10^{-3}$ m s^{-1}. Key: (◊) $a = 0.008$ m and (+) $a = 0.002$ m.

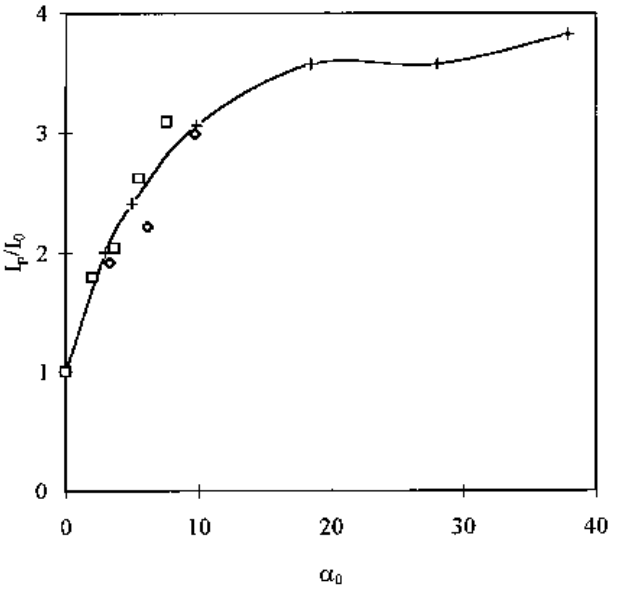

Fig. 9. Variation of I_p/I_0 against the dimensionless velocity, α_0, for different values of the fluid velocity. $a = 8\times10^{-3}$ m. Key: (+) $v = 1.33\times10^{-3}$ m s^{-1}, (◊) $v = 3.98\times10^{-3}$ m s^{-1} and (□) $v = 6.63\times10^{-3}$ m s^{-1}.

the steady velocity increases, and remains constant with the pulsation amplitude.

However, the results shown in Figs 9 and 10 can be explained from the theoretical variation of the wall shear stress in an annular pulsating flow studied by Pérez-Herranz [32]. This author has found that for a given value of α_0, it is better to increase frequency than to increase amplitude in order to get a higher increase in the relative variation of the shear stress on the inner wall of the annulus and so the effect of frequency on the limiting current must be higher than the effect of amplitude.

3.3. *Relative variation of mass transfer in pulsating flow*

It is usual to correlate the relative variation in mass transfer in terms of the dimensionless groups characterizing the pulsating flow. These dimensionless groups are the dimensionless velocity, α_0, and the Stokes number, α_1, defined by Equations 1 and 2, respectively. Krasuk and Smith [24] found theoretically that the effect of pulsating flow on mass transfer in a pulsed column can be correlated using an expression of the form:

$$\frac{Sh_p - Sh_0}{Sh_0} = A(\alpha_0\alpha_1)^B \tag{3}$$

where A and B are constants.

This expression was used by Krasuk and Smith [27] and by Ratel *et al.* [28] in the experimental study of mass transfer in packed beds in pulsating flow, where Sh_p is the time-averaged Sherwood number in pulsating flow and Sh_0 is the Sherwood number in steady state. These Sherwood numbers are calculated from the value of the limiting current using the expression:

$$Sh = \frac{I_{lim}D_{eq}}{SzFDC_0} \tag{4}$$

where the symbols are as defined at the outset of this paper.

Assuming that the effect of pulsating flow on the mass transfer for an annulus can be represented using Expression 3, we obtained the following correlation from the least squares fit of the experimental data:

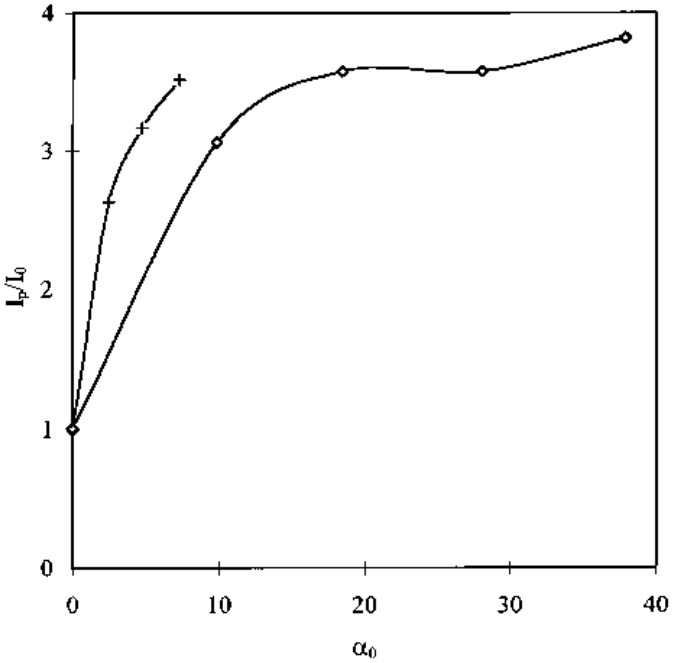

Fig. 10. Variation of I_p/I_0 against the dimensionless velocity, α_0, for different values of amplitude. $v = 1.33\times10^{-3}$ m s^{-1}. Key: (+) $a = 0.002$ m and (◊) $a = 0.008$ m.

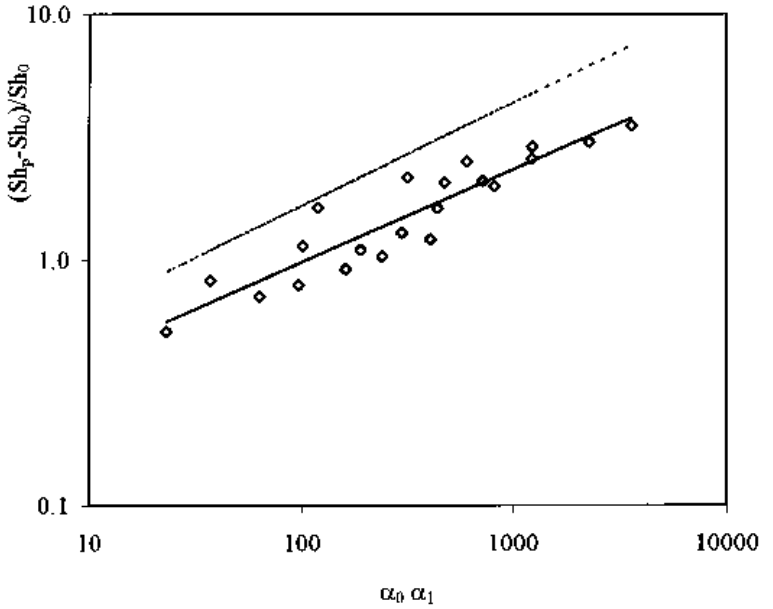

Fig. 11. Fractional increase in the Sherwood number due to pulsations. Key: (◊) experimental data; (——) least square fit of the experimental data (Equation 5); (- - -) Krasuk and Smith correlation (Equation 6).

$$\frac{Sh_p - Sh_0}{Sh_0} = 0.192(\alpha_0\alpha_1)^{0.377} \qquad (5)$$

Figure 11 shows the relative variation of the experimental Sherwood number calculated from Equation 4 with the product of the pulsation parameters, α_0 and α_1, and the least squares fit of the data in pulsating flow given by Equation 5. This equation is similar to that found by Krasuk and Smith [27] for mass transfer in a packed bed in pulsating flow:

$$\frac{k_p - k_0}{k_0} = 0.24(\alpha_0\alpha_1)^{0.42} \qquad (6)$$

where k_p is the time-averaged mass transfer coefficient in pulsating flow and k_0 is the mass transfer coefficient in steady flow. In Fig. 11 Equations 5 and 6 are compared, showing a good agreement. The difference in the constants of the second terms in Equations 5 and 6 are due to the additional contribution of the packing to the hydrodynamics in the work of Krasuk and Smith [27].

Acknowledgements

We wish to express our gratitude for the support of this work by the D.G.I.C.Y.T. (convention no. PB93-0379). We thank María Asunción Jaime for her help in translating this paper into English.

References

[1] M. Boudet-Dummy, A. Lindheimer and C. Gavach, *J. Memb. Sci.* **57** (1991) 57.
[2] R. Audinos. 'Separation and Purification Technology', Marcel Dekker, New York (1994).
[3] B. R. Noh. *Ind. Eng. Chem. Prod. Res. Dev.* **20** (1981) 170.
[4] T. C. Huang and R. S. Juang, *ibid.* **25** (1986) 537.
[5] A. T. Cherif and C. Gavach, *Hydrometallurgy* **21** (1988) 191.
[6] V. Baltazar, G. B. Harris and C. W. White, *ibid.* **30** (1992) 463.
[7] V. P. Greben, N. Y. Pivovarov, Y. G. Rodzik and N. Y. Kovarskii, *J. Appl. Chem. USSR* **65** (1992) 619.
[8] R. Audinos, A. Nassr-Allah, J. R. Alvarez, J. L. Andrés and R. Alvarez, *J. Memb. Sci.* **76** (1993) 147.
[9] G. Pourcelly, Y. Tugas and C. Gavach, *J. Memb. Sci.* **97** (1994) 99.
[10] V. P. Greben, N. Y. Pivovarov, Y. G. Rodzik and N. Y. Kovarskii, *J. Appl. Chem., USSR* **64** (1991) 709.
[11] A. Lindheimer, M. Boudet-Dummy and C. Gavach, *Desalination* **94** (1993) 151.
[12] L. Liao, A. Van Sandwijk and G. Van Weert, *J. Appl. Electrochem.* **25** (1995) 1009.
[13] T. Yoshihara. *Japanese patent Kokai Nosho. 53 96 994* (1978).
[14] J. Catonne and J. Royon, *Trait. Surf.* **165** (1978) 35.
[15] J. L. Eisenmann, 'Membrane processes for Metal Recovery from Electroplating Rinse Water'. Second Conference on Advanced Pollution Control for the Metal Finishing Industry, E.P.A. Cincinaty, OH (1979) 99.
[16] T. Cohen and F. Duclert, *R.G.E.* **3** (1992) 17.
[17] T. C. Huang, *J. Chem. Eng. Data* **22** (1977) 422.
[18] R. Audinos, *Electrochim. Acta* **25** (1988) 193.
[19] T. C. Huang and I. Y. Yu, *J. Memb. Sci.* **35** (1988) 193.
[20] T. C. Huang and J. H. Wang, *Can. J. Chem. Eng.* **67** (1989) 385.
[21] H. Gibert and H. Angelino, *ibid.* **51** (1973) 319.
[22] *Idem, Int. J. Heat Mass Transf.* **17** (1974) 625.
[23] J. L. Guiñón, V. Pérez-Herranz, J. García-Antón and G. Lacoste, *J. Appl. Electrochem.* **25** (1995) 267.
[24] J. H. Karasuk and J. M. Smith, *Chem. Eng. Sci.* **18** (1963) 591.
[25] M. R. Mackley and X. Ni, *ibid.* **46** (1991) 3139.
[26] S. T. L. Harrison and M. R. Mackley, *Chem. Eng. Sci.* **47** (1992) 490.
[27] J. H. Krasuk and J. M. Smith, *A.I.Ch.E.J.* **10** (1964) 759.
[28] A. Ratel, P. Duverneuil and G. Lacoste, *J. Appl. Electrochem.* **18** (1988) 394.
[29] F. Coeuret and M. Paulin, *ibid.* **18** (1988) 162.
[30] D. A. Cowan and J. H. Brown. *Ind. Eng. Chem.* **51** (1959) 1445.
[31] S. Uchida, *Zamp.* **7** (1956), 403.
[32] V. Pérez-Herranz, PhD, dissertation, Universidad Politécnica de Valencia. Spain (1994)
[33] J. M. Khodadadi, *J. Fluid Eng.* **113** (1991), 509.
[34] L. Meites, Polarographic Techniques, John Wiley, New York (1965).
[35] O. E. Karamercan and J. L. Gainer, *Ind. Eng. Chem. Fundam.* **18** (1979) 11.